Characterizing the Distribution of Methane Sources and Cycling in the Deep Sea via in Situ Stable Isotope Analysis

Scott D. Wankel,*[†,‖] Yi-wen Huang,[‡,⊥] Manish Gupta,[§] Robert Provencal,[§] J. Brian Leen,[§] Andrew Fahrland,[§] Charles Vidoudez,[‡] and Peter R. Girguis*[‡]

[†]Department of Earth and Planetary Sciences, Harvard University, Cambridge, Massachusetts 02138, United States
[‡]Department of Organismic and Evolutionary Biology, Harvard University, Cambridge, Massachusetts 02138, United States
[§]Los Gatos Research, Inc., Mountain View, California 94041, United States

Ⓢ Supporting Information

ABSTRACT: The capacity to make in situ geo-referenced measurements of methane concentration and stable isotopic composition ($\delta^{13}C_{CH4}$) would greatly improve our understanding of the distribution and type of methane sources in the environment, allow refined determination of the extent to which microbial production and consumption contributes to methane cycling, and enable the testing of hypotheses about the sensitivity of methane cycling to changes in environmental conditions. In particular, characterizing biogeochemical methane cycling dynamics in the deep ocean is hampered by a number of challenges, especially in environments where high methane concentrations preclude intact recovery of undisturbed samples. To that end, we have developed an in situ analyzer capable of $\delta^{13}C_{CH4}$ measurements in the deep ocean. Here we present data from laboratory and field studies in which we characterize the instrument's analytical capabilities and performance and provide the first in situ stable isotope based characterization of the influence of anaerobic methane oxidation on methane flux from seep sediments. These data illustrate how in situ measurements can permit finer-scale analyses of variations in AOM activity, and facilitate advances in using $\delta^{13}C_{CH4}$ and other isotopic systems to interrogate biogeochemical cycles in the deep sea and other remote or challenging environments.

1. INTRODUCTION

Since some of earliest concentration measurements of methane (CH_4) in the ocean,[1-4] our understanding of the marine methane budget and its role in the global climate system has greatly evolved, providing important insights into the dynamics of this important greenhouse gas (reviewed by 5). We now understand that marine sediments harbor the largest single source of methane production (methanogenic archaea), and geochemical and microbiological studies have also provided evidence for the importance of anaerobic oxidation of methane (AOM) by microbes as a primary regulator of sedimentary methane flux to the ocean and atmosphere (reviewed by 6). While the importance of AOM in regulating methane flux from marine sediments to the atmosphere is undisputed, the precise nature of AOM is still the topic of intense investigation.

To date, study of the marine methane cycle has, to some degree, been hindered by the difficulties of studying dissolved gases in the deep ocean. Isobaric (pressure-retaining) samplers are typically used for targeted sample collection from prominent features (e.g., hydrothermal vents) and are impractical for broad spatial characterization of deep ocean environments. Fluids collected by samplers without the ability to retain pressure generally suffer from outgassing due to depressurization during recovery, which confounds interpretation. Recent advances in underwater mass spectrometry and other analytical instruments have overcome many of the challenges of quantifying dissolved volatiles in situ.[7-12] For example, in situ methane concentration profiles collected via an in situ mass spectrometer within a Gulf of Mexico brine pool constrained diffusive methane fluxes from these systems, and in conjunction with shipboard rate measurements established that AOM rates are approximately 2 orders of magnitude higher than previously documented.[12] In situ mass spectrometry has also been used to determine the physical, chemical, and biological processes controlling the fate of methane (and other hydrocarbons) derived from the Macando well accident,[13] and to monitor the relationships among oxygen, carbon, and nitrogen cycling in coastal waters.[7,8] These advanced in situ analytical platforms continue to enable the discovery of important aspects of processes operating in marine systems

over a wide range of spatial scales from cm[11,12] to m[7,11] to km.[13]

In many cases, however, chemical composition alone provides a limited perspective on the underlying processes responsible for an observed distribution. In general, concentration only reflects the net effect of biological and abiotic production and consumption, and it is often difficult to gain information about rates of transformations, types of processes, and magnitude of fluxes. However, because of inherent differences in the relative reaction kinetics of naturally occurring stable isotopes (e.g., ^{12}C vs ^{13}C), stable isotope ratios offer a more robust means of disentangling the effects of multiple processes, revealing the nature and relative contributions of the biological, chemical, and physical phenomena underlying a realized concentration. Stable isotope analysis has proven to be an invaluable (bio)geochemical tool across all types of environments as well as spatial and temporal scales.[14−17]

Although isotope ratio mass spectrometry (IRMS) is the standard method for such isotopic analyses, the associated infrastructure has generally precluded its adaptation for field use. Recent advances in laser absorption spectroscopy techniques (e.g., optical spectroscopy), including tunable diode laser (TDLAS), cavity ring-down (CRDS), and off-axis integrated cavity output (ICOS) spectroscopy, are practical alternatives to IRMS in many applications including routine laboratory analyses of isotopologues of H_2O,[18−21] CO_2,[18−21] CH_4,[22,23] N_2O,[24−26] and organic compounds.[27] These systems are typically smaller in size, consume less power, and occupy less space. They are capable of isotope ratio measurements with accuracy and precision that rivals conventional IRMS.[21,26,32] Further, because of their relaxed operational constraints, laser-based systems are far better suited to field deployments. To date, successful field deployments of laser-based instruments have been used to study water isotope dynamics in the tropical tropopause,[28] the temporal dynamics of forest respiration,[29] and rain/snow mixing patterns,[30] as well as fine-scale variations in dissolved CH_4 and CO_2 in surface waters of the Baltic Sea,[31] among other studies.

The development of an in situ stable isotope analysis platform for use underwater would enable rapid, higher resolution (spatial and temporal) analyses, which are needed to provide more robust constraints on the relative influences of biological, geochemical, and physical processes influencing marine biogeochemical budgets. To that end, we have developed a deep-sea in situ analyzer, based on off-axis integrated cavity output spectroscopy (ICOS), that is capable of measuring methane stable carbon isotope ratios (^{13}C:^{12}C) in near real-time, at water depths up to 3000 m. Here we present the instrument design, as well as laboratory experiments and calibrations designed to characterize the influence of environmental conditions on measurement accuracy. Moreover, we present the first in situ measurements of $\delta^{13}C_{CH4}$ from cold seeps in Monterey Bay, which provide in situ characterization of the efficiency of AOM at a hydrocarbon seep, and serve to illustrate the utility of in situ $\delta^{13}C_{CH4}$ measurements for improving constraints on methane biogeochemical cycling in the deep sea.

2. MATERIALS AND METHODS

2.1. Instrument Design and Configuration. Figure 1 shows a schematic of the layout and major systems of the in situ ICOS analyzer. The fundamental principles of the off-axis
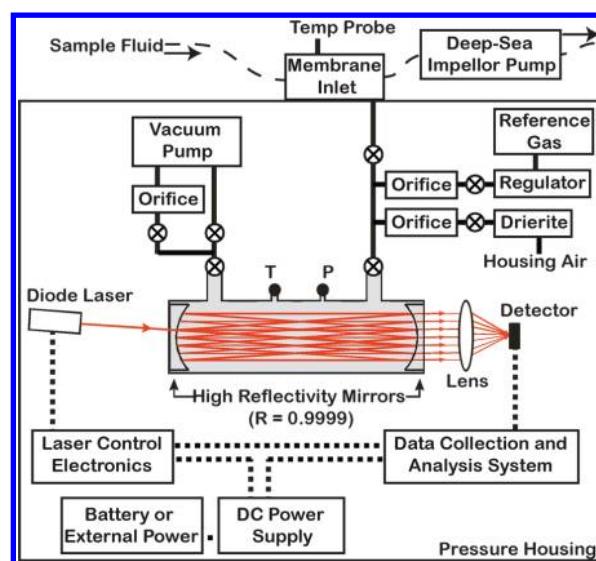

Figure 1. Schematic of instrument layout illustrating external fluid pumping system (dashed lines), internal gas phase transfer and vacuum pumping system (solid lines), and electrical systems (dotted lines). All gas phase and electrical systems are housed within a titanium pressure housing rated to 3000 m depth.

ICOS analyzer have been described elsewhere.[32] Briefly, the cavity consists of a 28-cm long, 5-cm diameter cell bounded by two highly reflective mirrors (reflectivity = 99.9929%). The cell is equipped with a pressure gauge and thermistor to provide accurate readings of gas pressure and temperature in the cell (±0.1 Torr and ±10 mK, respectively). A distributed feedback (DFB) diode laser operating near 1648 nm is coupled into the cavity in an off-axis fashion and light transmitting through the cavity is focused onto an amplified InGaAs detector whose signal is digitized, analyzed, and stored by an onboard computer. The laser, which is mounted onto a custom driver that controls the current and temperature, is current-tuned over ~2 cm^{-1} (60 GHz). Transmission spectra (62) are averaged together to provide a single spectrum that is stored to disk for postanalysis, yielding a net data rate of 1 Hz. The acquired spectra are then analyzed using a chemometric data anlaysis routine. Ninety-seven such analyses are performed per measurement to yield a single $\delta^{13}C_{CH4}$ value. The acquired spectra are then analyzed using a chemometric data analysis routine.[33,34]

Although based on a "conventional" ICOS analysis platform, this instrument has been specially configured to fit into a cylindrical pressure housing and designed to extract dissolved sample gases through a membrane inlet, deliver that gas into the analytical cell, and compare analyses to "onboard" isotope reference standards. The membrane inlet through which dissolved gases are introduced has been previously described.[11,12] Approximately 2 cm^2 of Teflon AF 2400 membrane backed by a layer of polyvinylidene fluoride is supported by a stainless steel frit (5 μm pore size) and separates the external fluid flow path from the internal analyzer vacuum chamber. For sampling, seawater is continuously pumped though this inlet at flow rates ranging from 50 to 250 mL/min (see below). A customized gas handling system comprising miniature solenoid valves, pressurized gas cylinders, and regulators for isotope reference standards and an "onboard" vacuum pump (KNF Neuberger, Inc.) are used to transfer sample and reference gases within the instrument and

to control vacuum pressure within the measurement cell. A 6Al4V titanium housing, 20.4-cm diameter × 119.6-cm long, houses the instrument and is rated to 3000 m (KUM GmbH, Kiel, Germany).

Sequentially, a gas sample is extracted through the membrane inlet, after which a series of software-controlled solenoid valves is operated to transfer an aliquot of sample gas into the ICOS cell (Figure 1). Next, the ICOS cell is slowly pumped down to a vacuum pressure of 10 Torr, followed by measurement for 60 s. Measurement of each sample $^{13}C:^{12}C$ is independently referenced to a periodic internal analysis of known reference gas to correct for any drift due to changes in electronic gain or sensitivity, or ambient conditions. Between each reference and sample analysis, the ICOS cell and transfer lines are purged with dry air or N_2 to eliminate carryover between sample and reference analyses. The measured transmission spectrum is then expressed as the sum of a baseline and absorptions due to $^{12}CH_4$ and $^{13}CH_4$. The fitted parameters include isotopologue concentrations and a spectral offset to account for slight shifts in the laser wavelength. The fit results provide absolute concentrations of $^{12}CH_4$ and $^{13}CH_4$ (ppm_v) and are used to calculate both methane concentration in the cell and carbon isotope ratio ($\delta^{13}CH_{CH4}$) expressed in permil (‰), where $\delta^{13}CH_4$ is equal to $[(^{13}R_{sample}/^{13}R_{VPDB}) - 1] *1000$ and R is the ratio of ^{13}C to ^{12}C in the sample and standard (VPDB), respectively. A more detailed description of the isotope reference scheme and analytical routine is given in the Supporting Information.

2.2. Lab Experiments. Stable isotope analyses are particularly susceptible to physical or chemical factors that discriminate against the heavier isotope (isotopic fractionation). The challenges associated with in situ measurements, including limited space within the pressure housing and—at times—limited power when running autonomously, present a formidable challenge to incorporating most laboratory-developed approaches. Thus, the goal of our laboratory-based characterization was both to gain a rigorous understanding of the behavior of the analyzer under operational conditions and to develop suitable operational approaches to minimize perturbations in situ and increase resolution and precision. To that end, we built a high-pressure, high-flow equilibration system (Figure 2) to characterize membrane inlet behavior across a wide range of conditions, including temperatures (2–25 °C), pressures (15–1500 psi), flow rates (0–200 mL/min), and concentrations (0.5 to ~18 mM CH_4). We describe the results of these experiments below, which provide a basis for interpreting the response and behavior of the membrane to various environmental conditions to provide the most accurate and reliable in situ measurements of $\delta^{13}CH_4$.

2.3. Calibration Approach. Calibration solutions were generated using a high-flow, high-pressure equilibration system (Figure 2). Briefly, water was circulated using a variable-flow control, high-pressure fluid pump (Lewa, Inc.). Fluids were circulated through a vertically oriented pressure cylinder, past the membrane inlet of the ICOS analyzer, and through a high-performance, corrosion-resistant fluid backpressure regulator (StraVal, Inc.; P/N BPH0502T) which was used to control hydrostatic pressure on the membrane inlet (BP1). Variable mixtures of CH_4 and N_2 were produced using high-precision mass flow controllers (Sierra Instruments, Inc.), the outflow of which was bubbled through the equilibration cylinder. Head-space pressure within this equilibration cylinder was controlled by a separate gas backpressure regulator (BP2) (Swagelok, Inc.;
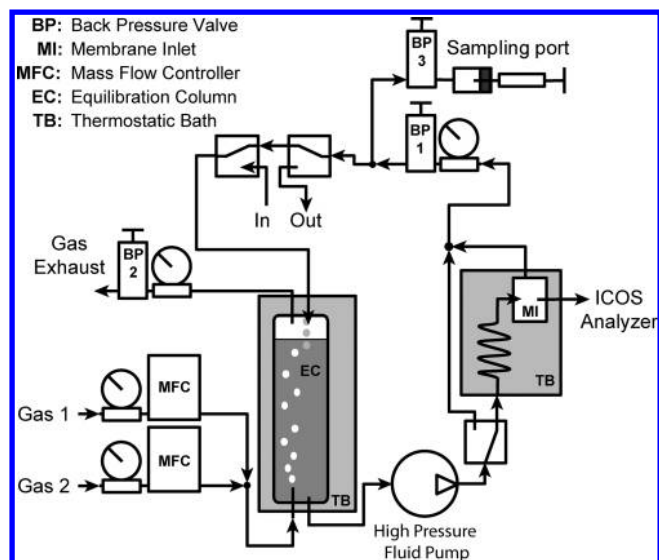

Figure 2. Schematic representation of the high-pressure equilibration system used for calibration of the in situ ICOS system. Gray boxes depict temperature-controlled baths kept at the same temperature. A high-pressure fluid pump is used to continually circulate fluids through the system at variable flow rates. Back-pressure regulators are used to control pressure in various parts of the system. BP1 is used to control the hydrostatic pressure felt by the membrane inlet (simulating deep ocean pressure). BP2 is used to control the headspace pressure of the equilibration chamber which influences dissolved CH_4 concentration. BP3 is used to drop pressure to allow sampling by gastight syringe for gas chromatographic analyses. Mass flow controllers were used to control the mixture of gases in the headspace (usually N_2/CH_4).

P/N SS-4R3A), which together with variable gas mixes was used to control CH_4 concentrations in the fluid. Finally, a third fluid/gas backpressure regulator (Swagelok, Inc.) was used to enable fluid (and gas) sampling (BP3) via a syringe sampling port for gas chromatographic analysis. Results were also compared and generally agreed well with calculated concentrations using published equations of state.[35] The equilibration cylinder, the membrane inlet, and all stainless steel tubing were contained within a thermostatic bath (±0.1 °C). Various factors (methane concentration, flow rate, hydrostatic pressure, and temperature) were manipulated to investigate their influence on the measurement of dissolved $\delta^{13}C_{CH4}$. For a given set of experimental conditions, a single ICOS-based $\delta^{13}C_{CH4}$ measurement (of one sample gas and one standard gas) was produced approximately every 5 min, with anywhere between 3 and 10 individual $\delta^{13}C$ measurements typically used to provide an estimate of external precision (e.g., reproducibility). In addition to the internal calibration gas used between each sample analysis, internal precision was also checked daily by internal measurement (e.g., not through the membrane inlet) of three commercially purchased isotope standards (Isometric Instruments; H-iso1 $\delta^{13}C = -23.9$‰; B-iso1 $\delta^{13}C = -54.5$‰; L-iso1 $\delta^{13}C = -66.5$‰).

2.4. Analyzer Deployments at Deep-Sea Hydrocarbon Seeps. Deployments described here were conducted aboard the R/V *Point Lobos* using the ROV *Ventana* (Figure S4), which supplies power (120VAC) and communications (CAT-5 Ethernet) to the instrument via standard deep-sea electrical connectors (SeaCon-Branter, Inc.). Two ROV dives with the in situ ICOS were conducted to the Extrovert Cliff seep fields within the Monterey Canyon (36° 46.6′ N, 122° 05.1′ W;

960−970 m water depth) during August and November of 2009. Typical ROV bottom times were 3−4 h, allowing up to 3 sites to be surveyed per dive. Most seeps were easily denoted by large radial colonies of clams (*Calyptogena* spp.) and visibly advecting fluids that emanated from a central seep orifice. Fluids were pumped from a sampling wand (3/8-in. stainless steel tubing) through flexible plastic tubing (Kel-F, McMaster-Carr) at a rate of ∼90 mL/min by a Seabird SBE-5 M submersible pump (Figure S4). By placing the tip of the sampling wand directly into the seep orifice, samples of advecting fluid for measurement of $\delta^{13}C_{CH4}$ were collected without disturbing the surrounding microbial mat or sediments. A temperature probe was used to record fluid temperature (4.16 ± 0.13 °C) at the membrane inlet (MISO Low-T probe, WHOI). When possible, 30-cm-long pushcores were also collected for sampling of porewaters for independent IRMS measurement of $\delta^{13}C_{CH4}$, microbial community analyses, and lab-based biogeochemical rate measurements (Wankel and Girguis, unpublished data). Immediately following the gentle removal of the pushcores, the ICOS sampling wand was placed ∼15 cm into the core hole for a measurement of porewater $\delta^{13}C_{CH4}$. Though fluids within these pushcore holes are not a quantitative measurement of porewater chemistry and will reflect a large influx of overlying seawater, we used this approach to gain some first-order perspective on the composition of $\delta^{13}C_{CH4}$ within sediment porewaters of these seeps.

3. RESULTS AND DISCUSSION

3.1. Laboratory Characterization. Below we discuss the results of the laboratory-based characterization of instrument performance, focusing on both internal (e.g., ICOS cell, sample size linearity, vacuum pressure, etc.) and external (e.g., membrane temperature, hydrostatic pressure, fluid flow rate, etc.) aspects, and their influence on the overall variability in the accuracy and precision of in situ measurements of $\delta^{13}C_{CH4}$.

3.1.1. Internal Instrument Performance. Several factors can contribute to variability in the measurement of methane $^{13}C:^{12}C$ within the ICOS cell including vacuum pressure (i.e., relative number of molecules contributing to absorbance features), ambient temperature (e.g., of the ICOS cell), and concentration. To determine if changes in temperature of the ICOS cell cause systematic variations in measured $^{13}C:^{12}C$, we analyzed a series of measurements across a range of temperatures both in the lab and during field deployments. While notable changes in the raw isotopologue concentrations (of reference gas) were observed at different temperatures, we observed that changes in temperature affected samples and standard gas identically (highlighting the utility of paired sample/standard analyses) and negate the effect of changing temperature on the internal ICOS performance.

Concentration of CH_4 in the cell can also influence the measurement of $^{13}C:^{12}C$, particularly at lower CH_4 concentrations (e.g., <800 ppm). Based on our assessments, a slight nonlinearity in the relationship between actual ^{12}C (and ^{13}C) and measured ^{12}C (and ^{13}C) concentrations is observed over a wide range, which was formalized and applied to the raw data (Figure S2). This "concentration effect" is empirically calibrated and corrected by the software for reporting of raw ^{12}C and ^{13}C concentrations of each sample and establishes a lower limit of CH_4 concentration at which $\delta^{13}C$ can be accurately measured (using this particular configuration; Figure 3). While this size correction also varies slightly with temperature, as long as at
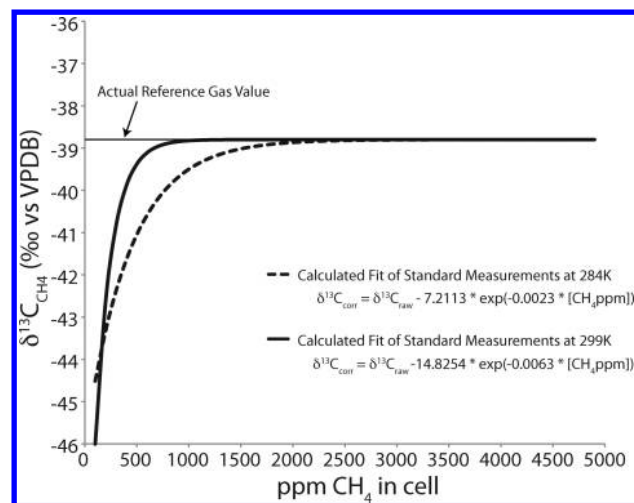

Figure 3. Results of calibration measurements conducted in environmental chamber at 284 and 299 K to illustrate both the sensitivity of $\delta^{13}C$ accuracy to amount of CH_4 in the optical cell and also the influence of temperature on this size dependence. Colder temperatures require more CH_4 to achieve the same accuracy as at higher temperatures. Exponential fit of this standard curve is used to adjust for a temperature specific concentration dependence of raw $\delta^{13}C$ values.

least two different basis sets can be gathered at temperatures that bracket those experienced during deployment, this secondary effect is easily removed. As seen in Figure 3, there is a minimum threshold CH_4 concentration above which a size effect becomes irrelevant. At the higher temperatures of the laboratory calibrations, $\delta^{13}C$ data was acceptable at CH_4 concentrations as low as 500 ppm. However, during the deep-sea deployments, due to the colder temperature of the ICOS cell, this lower threshold was closer to 1000 ppm (e.g., the level at which the error in the corrected $\delta^{13}C_{CH4}$ measurements exceeds our estimate of internal precision of ±0.8‰). It should also be noted that all samples measured during laboratory calibrations were analyzed at 7 Torr and were referenced to basis sets made at 10 Torr, which could lead to systematic errors. However, error propagation revealed that error induced by using basis sets taken under different ICOS cell pressures of this magnitude is at least an order of magnitude smaller than our estimate of precision and is therefore neglected.

In the lab, regular measurement of three isotope standards (H-iso1 $\delta^{13}C$ = −23.9‰; B-iso1 $\delta^{13}C$ = −54.5‰; L-iso1 $\delta^{13}C$ = −66.5‰) exhibited slopes (true $\delta^{13}C$ vs measured $\delta^{13}C$) ranging from 0.992 to 1.059 with an average standard error of 0.8‰ over the $\delta^{13}C$ range measured. Observed changes in this relationship likely stem from natural temperature variations in the lab during the day (a change of approximately this magnitude could be expected for a temperature shift from 19 to 26 °C, for example). Accounting for all these factors in aggregate, we report the internal precision of the $\delta^{13}C$ measured by this instrument as configured to be ±0.8‰.

Custom ICOS instruments are capable of measuring CH_4 concentration and carbon stable isotopic composition at CH_4 mixing ratios as low as ambient atmospheric CH_4 (1.8 ppm),[23] and commercially available benchtop instruments are now reporting similar capabilities.[36] The in situ isotope analyzer presented here is implicitly capable of making coregistered concentration measurements, though performance differs from

the benchtop instruments due to the use of a membrane inlet, differences in the optical bench, and the presence of water vapor in the cell (which influences the proportion of methane gas in the optical path). Based on controlled lab experiments, the currently configured analyzer is capable of concentration measurements down to ~100 μM $\pm$ 5% (with greater precision at higher concentrations), and accurate $\delta^{13}C_{CH4}$ values (see below) in fluids with methane concentrations as low as ~500 μM (leaving ambient CH_4 currently out of reach in its current configuration). As mentioned, the in situ ICOS analyzer was configured to pump water past the inlet at relatively high velocity as a simple and robust approach to dissipating boundary layers that can form at the inlet. As a consequence, such samples are admixtures of target fluids and background seawater that are not necessarily representative of in situ concentrations. Ongoing efforts are aimed at reconfiguring the inlet design to alleviate the need for rapid fluid pumping, and subsequently producing calibrations for dissolved CH_4 concentration with the new inlet system. When configured as such, the instrument will be well poised to quantify methane concentrations with sensitivity equal to or exceeding existing in situ mass spectrometers,[7,8,11] and provide coregistered determinations of $\delta^{13}C_{CH4}$.

3.1.2. Membrane Inlet Behavior. We also explored a range of external factors that potentially contribute to variability in the measurement of $\delta^{13}C_{CH4}$ resulting from isotopic fractionation during the transfer of methane into the ICOS instrument for analysis. The primary effects discussed below pertain to the physical−chemical processes responsible for transferring dissolved methane from the water sample through the semipermeable Teflon AF membrane. The process by which sample gas moves from a dissolved phase in sample fluids through the membrane and into gas phase for analysis is termed permeation (also called pervaporation),[37−39] which is the combination of three physical−chemical processes: (1) sorption of gas molecules onto the surface of the membrane, (2) diffusion (or permeation) of molecules through the membrane, and (3) desorption of gas molecules from the back of the membrane into the vacuum chamber of the instrument. We manipulated fluid flow rate, fluid and membrane temperature, and hydrostatic pressure to determine the relative importance of these environmental parameters on the magnitude of isotopic fractionation due to changes in permeation through the membrane.

3.1.2.1. Flow Rate. Tests were conducted using fluids of constant methane concentration and $\delta^{13}C_{CH4}$ while changing flow rates through the inlet housing. Observed responses in measured $\delta^{13}C_{CH4}$ values indicated isotopic fractionation due to both boundary layer formation at low flow and changes in methane sorption onto and/or diffusion through the membrane with increasing flow. Figure 4 shows the changes in $\delta^{13}C_{CH4}$ analyzed over a range of flow rates through the membrane inlet housing. At low flow, extremely high variability is observed consistent with boundary layer formation at the membrane surface, in which a very small and quasi-isolated pool of dissolved CH_4 is fractionated during permeation through the membrane (e.g., 39). Under low flow, fluid turbulence is insufficient to disrupt boundary layer formation. The composition of this small pool is quickly altered, giving $\delta^{13}C_{CH4}$ values with no obvious relation to the composition of methane in the outside fluid. By increasing flow rates to >60 mL/min, boundary layer formation is disrupted and $\delta^{13}C_{CH4}$ measurements stabilize. Under turbulent flow, the apparent
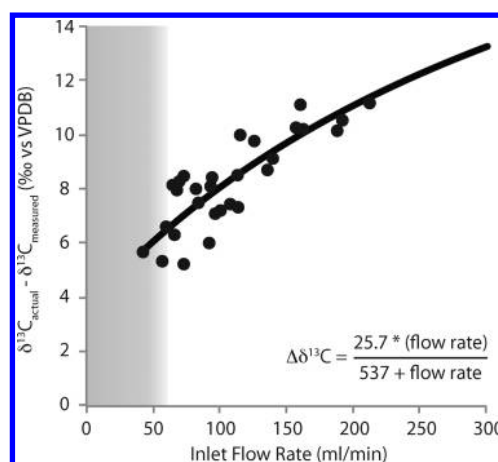

Figure 4. Influence of fluid flow rate on apparent isotope effect imparted by transfer of methane through the membrane into the analyzer. At flow rates <50 mL/min (gray area) boundary layer formation leads to erratic $\delta^{13}C_{CH4}$ values.

isotopic fractionation (e.g., the difference between the true $\delta^{13}C_{CH4}$ and that measured within the analyzer; $\Delta\delta^{13}C$ or $\varepsilon_{mem-app}$) is manifest as the net effect of fractionation due to sorption of CH_4 onto the membrane surface, diffusion of CH_4 through the membrane, and desorption of methane on the vacuum side of the membrane. Sorption of CH_4 molecules onto the membrane surface involves the formation of weak (van der Waals) bonds, while diffusion involves molecular interactions with the polymer during movement through the membrane. Such physical−chemical processes are commonly known to result in isotopic fractionation since the rate of interaction between the membrane surface and $^{12}CH_4$ isotopologues will proceed more rapidly than $^{13}CH_4$. While recent work has explored isotope fractionation of water vapor and CO_2 during permeation across semipermeable membranes,[21,40,44] to the best of our knowledge, the data presented here are the first to examine the isotope effects of CH_4 permeation.

In general the net process of permeation, like diffusion, is not unidirectional and represents a net balance between the flux of gas permeating into and back out of the membrane under steady-state conditions. Empirically, we observed an increase in $\varepsilon_{mem-app}$ as flow rate increased (Figure 4), consistent with an increase in the relative importance of sorption onto the membrane surface (related to the effect of physical shear of fluid flow) and/or a change in the reversibility of permeation through the membrane (e.g., return flux out of the membrane relative to the flux into the analyzer; see Supporting Information). At high flow rates, mass balance indicates a higher degree of reversibility. In practice, the observed isotope effect ($\varepsilon_{mem-app}$) will reflect the mass-weighted balance of these two processes (and any isotope effects). Although further constraint of the physical nature of this process is beyond the scope of this work, our interpretation suggests that an increase in flow rate increases the apparent isotope discrimination ($\varepsilon_{mem-app}$). For the purposes of correcting these effects for in situ measurements, we determined the value of $\varepsilon_{mem-app}$ empirically, under in situ sampling conditions, through laboratory calibration (see below).

3.1.2.2. Hydrostatic Pressure and Fluid Temperature. Given the demonstrated changes in the magnitude of isotopic fractionation due to variations in flow rate, we hypothesized that hydrostatic pressure and temperature would also exert

considerable influence over the behavior of the membrane material and isotopic fractionation. Temperature should directly influence both the degree of molecular sorption onto the membrane surface and the diffusion coefficients for each isotopologue, while high hydrostatic pressure is known to cause porespace deformation in many materials.[41] A matrix of conditions was evaluated using a fixed flow rate of ~100 mL/min while allowing temperature and hydrostatic pressure to vary, while continually measuring $\delta^{13}C_{CH4}$ through the membrane inlet. Figure 5 summarizes the measurements from
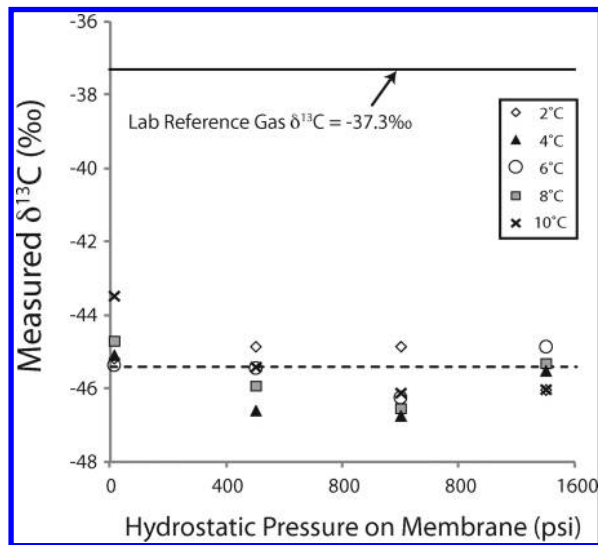

Figure 5. Results of laboratory calibrations using high CH_4 solutions over a range of temperature and hydrostatic pressures. While no relationship with measured $\delta^{13}C_{CH4}$ was found over the range of pressures and temperatures tested, a notable offset from the reference tank $\delta^{13}C_{CH4}$ value ($-37.3‰$) was consistently observed as a result of isotopic fractionation during permeation through the membrane.

the matrix of twenty test conditions (pressure = 1, 34, 68, and 102 atm; temperature =2, 4, 6, 8, and 10 °C) with each data point representing between 3 and 10 individual measurements. Measured $\delta^{13}C_{CH4}$ values for each set of conditions ranged from -46.8 to $-43.5‰$ with standard deviations of each condition ranging from 0.3 to 2.5‰. Overall, the approximately 350 measurements yielded an average value of $-45.6‰$ with a mean standard deviation of 1.2‰ (e.g., external precision). Surprisingly, no significant relationships were observed between $\delta^{13}C$ and hydrostatic pressure or temperature. While these experiments demonstrated very little variation among the different experimental (and in situ) conditions, they revealed a consistent offset of 8.3‰ from the reference CH_4 value of $-37.3‰$. We conclude that measurements made using a flow rate of ~100 mL/min result in an offset of 8.3 ± 1.2 ‰ over the range of temperatures and hydrostatic pressures evaluated. In total, we estimate our analytical accuracy based on these internal and external calibrations to be within ±2.3‰ when no explicit temperature- or pressure-related corrections are applied for temperatures between 2 and 10 °C and pressures between 1 and 102 atm. When in situ sampling occurs under relatively constant conditions, instrument precision is ±1.2‰ (as is the case in the field deployments below).

3.2. In Situ Field Data. Two deployments of the in situ ICOS analyzer were conducted in August and November of 2009 to methane seeps in Monterey Bay[42,43] at a site called

Extrovert Cliff (water depth ~962 m). Fluid seepage at Extrovert Cliff is primarily thought to be the result of an overpressured confined aquifer with flow channeled upward through permeable fractures.[44] In this environment, seafloor expressions of methane seepage are manifest by concentric rings of chemosynthetic microbes and clams surrounding a central seep orifice (e.g., 45). Radial mats of white−yellow sulfur-oxidizing bacteria were observed surrounding the immediate seep orifice and extending up to 40 cm away from the center. Beyond the microbial mats were dense colonies of *Calyptogena* clams extending several meters away from the center of the seep. At the very center of the seep, advective flow was usually noted by slight changes in water density (i.e., "schlieren" effect) and visibly moving filaments of bacterial mats. By placing the sampling wand directly into readily discernible fluid flow, measurements of the $\delta^{13}C_{CH4}$ of advecting fluids were taken over a period of typically 10−30 min, allowing for 2−10 individual measurements to be made. Because all samples were collected at the same depth and temperature (±0.2 °C), relative differences among sites and sample fluids are more robust than absolute accuracy of $\delta^{13}C_{CH4}$ values and are limited only by our analytical precision of ±1.2‰.

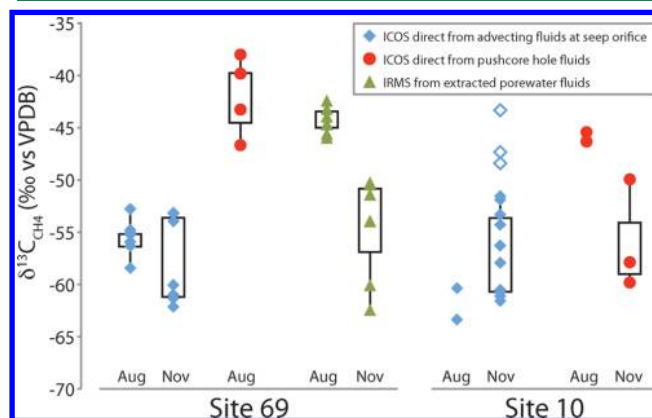Two primary seep sites (Sites 10 and 69), separated by <50 m, were sampled during both deployments (Figure 6). The

Figure 6. Methane carbon stable isotopic composition ($\delta^{13}C_{CH4}$) measured via the in situ ICOS analyzer. For comparison, extracted porewaters were also measured via conventional isotope ratio mass spectrometry (IRMS). Seep sites (69 and 10) were sampled during Aug and Nov 2009. Boxes denote range of two standard deviations centered on average value for data shown. Hollow symbols note statistical outliers and were omitted from statistical analysis. The high degree of variability observed by in situ ICOS between fluids sampled directly from the seep orifice and those sampled from within freshly pulled pushcore holes is confirmed by the IRMS analyses of extracted porewaters.

nature of sampling such an environment with the relatively high flow intake (~100 mL/min) from the sampling wand meant that our sample fluids likely contained large amounts of background seawater and were not chemically representative of "pure" seep fluid. However, during sampling of corehole fluids, methane-enriched fluids were readily apparent: levels of CH_4 inside the optical cell were always elevated by orders of magnitude in comparison to water column levels (e.g., >1000 ppm as compared with <2 ppm). Nevertheless, because the amount of methane contained in background seawater is generally quite low (nM) and CH_4 concentrations in seep fluids

are quite high (mM), the methane isotopic composition of the mixture between seawater and seep fluids is indistinguishable from pure seep fluids. Advecting fluids exhibited $\delta^{13}C_{CH4}$ ranging from −63.4 to −51.6‰ (Figure 6) (see Supporting Information for explanation of the corrections to the raw field data). Average $\delta^{13}C_{CH4}$ in advecting fluids measured from Site 10 during August and November were −61.9 ± 2.1 and −56.9 ± 4.0‰, respectively, while values for Site 69 were −56.0 ± 1.7 and −57.8 ± 4.2‰, respectively (Figure 6). Previously published porewater $\delta^{13}C_{CH4}$ values from Monterey Bay range widely (−30.6 to −86.6‰[43]), and our measurements fall within the range of values previously observed at those seeps located within the Monterey Bay fault zone (−49.1 to −53.6‰[43]) and are consistent with methane deriving from a mixture of both microbial and thermogenic sources (from the hydrocarbon-bearing Monterey Formation).

Sediment pushcores (∼20 cm deep) were taken from both sites, and immediately upon removal of the sediment core, the in situ ICOS sampling wand was placed into the vacant core hole (∼15 cm) to measure the $\delta^{13}C_{CH4}$ of the pore fluids emanating from the sides of the core hole (Figure 6). While CH_4 concentration measurements are generally uninformative in this configuration (due to some dilution with seawater induced by pumping and the rapid displacement of the sediments), the $\delta^{13}C_{CH4}$ measured primarily reflects the composition of the porewaters from the withdrawn sediment core and surrounding sediments due to the far lower CH_4 concentrations in the overlying water. Core hole fluids contained methane with generally higher $\delta^{13}C_{CH4}$ than advecting fluids and ranged from −59.8 to −38.0‰. Fluids from sediment core holes taken in August 2009 (at both sites) exhibited considerably higher $\delta^{13}C$ values than the fluids advecting from the seep orifice, while fluids in the November 2009 core hole at site 10 were more similar to advecting fluids. The observation of lower $\delta^{13}C$ values in advecting methane compared with shallow pore fluids and/or hydrate associated methane is generally reflective of the influence of anaerobic oxidation of methane (AOM) occurring above the sulfate−methane transition zone.[46,47] Higher $\delta^{13}C_{CH4}$ values are expected to result from AOM in sediments as the consumption of CH_4 by anaerobic methanotrophy results in a preferential utilization of the lighter isotopologue ($^{12}CH_4$) and an increase in the $\delta^{13}C$ of the remaining methane, with an isotope effect (ε_{AOM}) of up to 17‰ reported in sediment systems.[46,48,49]

For comparison, sediment cores from Site 69 (one each for Aug and Nov 2009) were sectioned and allowed to equilibrate with an anaerobic headspace in sealed bottles in the dark at 7 °C. After 24 h a 4-mL sample of the headspace gas was pulled via gastight syringe and injected into He-sparged exetainers for lab-based IRMS analysis of $\delta^{13}C_{CH4}$ (Figure 6). Duplicate IRMS analyses were within 0.1‰. $\delta^{13}C_{CH4}$ values from these two cores ranged from −62.4 to −43.2‰. Notably, the core from Aug 2009 showed a more evenly distributed and relatively higher $\delta^{13}C_{CH4}$ composition across sediment sections (−46.0 to −43.2‰), while the core from Nov 2009 exhibited a more vertically structured composition with a wider range of values having much lower $\delta^{13}C$ values (−62.4‰ near the surface up to −50.3‰ at 25 cm depth). The wider range and vertical structure of $\delta^{13}C_{CH4}$ values observed in this pushcore comprise the isotopic record of active microbial methane cycling occurring across the depths sampled by the sediment core, including the potential influence of both methanogenesis and AOM.

These two sample cores reflect the laterally heterogeneous nature of $\delta^{13}C_{CH4}$ distribution within the shallow subsurface of such seep environments. The extracted porewaters from August reflect the influence of AOM and are consistent with the contemporaneous core hole fluids as measured via in situ ICOS. However, the extracted porewater fluids from November appear to more closely reflect the composition of fluids advecting from the central seep orifice. Thus, while the IRMS analyses of extracted porewater $\delta^{13}C_{CH4}$ serve to illustrate and emphasize the inherent subsurface variability in seep hydrology and biogeochemistry, the range of $\delta^{13}C$ values measured remains in good agreement with those measured via in situ ICOS and confirms its performance in this deep-sea application.

As a further demonstration of the utility of in situ ICOS, we used a simple one-box model to make a first-order estimate of the relative "efficiency" of methane oxidized during diffusion of seep-derived methane through the surrounding sediments. Assuming that the $\delta^{13}C_{CH4}$ of fluids sampled directly from the seep orifice is representative of the composition of CH_4 diffusing into the reactive sediment zone ($\delta^{13}C_{seep}$), and the $\delta^{13}C_{CH4}$ of fluids measured in freshly pulled pushcore holes represents the steady state porewater composition in the near-surface sediments ($\delta^{13}C_{pw}$), a simple isotope mass balance model gives

$$\delta^{13}C_{pw} = \delta^{13}C_{seep} + f(\varepsilon_{AOM})$$

where ε_{AOM} is the fractionation by anaerobic oxidation of methane (we adopt a value of 17‰ based on published data)[46,48−50] and f is the fraction of methane consumed by AOM during diffusive transport—or the 'efficiency' of the sediment-hosted removal of methane (Table S1). Because any "contamination" in the core hole fluids by "unadulterated" seep fluids (e.g., if the pushcore intersected the main seep conduit) would act to decrease $\delta^{13}C_{pw}$ and lower estimates of f, this number reflects a lower estimate on methane oxidation efficiency. Table S1 shows that estimates of methane oxidation efficiency are generally greater than 83%. As mentioned above, sampling of site 10 during November resulted in corehole fluids that were indistinguishable from advecting fluids. This similarity in composition (likely due to the intersection of the pushcore with the subsurface conduit) results in a very low calculated value of AOM efficiency. Such in situ observations can be used to improve constraints on the value of ε_{AOM} within these sediments. To date, estimates for ε_{AOM} in sediments, calculated through a variety of modeling approaches, have ranged between 4 and 19‰.[46,48−50] Since values <16‰ would violate our isotope mass balance in three out of four cases, we suggest that the apparent values of ε_{AOM} in this environment are likely near the high range of those estimated by others (e.g., 50−52). We caution that variability in the observed composition of core hole fluids likely reflects the perturbations caused by the sudden removal of a volume of sediment from the seep surface. Not only is the underlying fluid hydrology unknown, but the act of pushing the sediment core into the sediment and then withdrawing the volume of sediment acts to disrupt the environmental equilibrium. Hence it is likely that samples of core hole fluids represent variable mixtures of advective fluids from some subsurface conduit and pore fluids from the surrounding sediments. Although the limited nature of our sampling approach does not consider vertical spatial resolution and the potential influence of methanogenesis, future refine-

1484

dx.doi.org/10.1021/es303661w | Environ. Sci. Technol. 2013, 47, 1478−1486

ments in methodology—including the implementation of a slower pumping system as well as a sediment porewater probe—should permit less invasive sampling and a better assessment of in situ $\delta^{13}C_{CH4}$ and concentrations profiles.

3.3. Ongoing Research and Development. The data herein demonstrate the efficacy of the in situ ICOS analyzer as an effective platform for the analysis of $\delta^{13}C_{CH4}$ within deep-sea environments, and consequently across a wide range of applications. For example, monitoring of changes in $\delta^{13}C_{CH4}$ could provide a more sensitive means for early detection of important changes in subsurface tectonic activity (e.g., prediction of earthquake/eruptions). Integration into tidal/coastal/continental shelf observatories would enable monitoring of biogeochemical dynamics in real-time, as is already being done with more conventional sensors.[53] Networked across fragile ecosystems rich in sediment-hosted methane, such as Arctic continental shelves,[54] ICOS technology could provide real-time feedback and help to constrain the timing and dynamics of ecosystem level fluxes and reaction mechanisms. Applications of ICOS will benefit from ongoing improvements in sensitivity. Current development efforts are aimed at improving performance through the removal of water vapor (thus increasing the proportional concentration of methane in the ICOS cell). In addition, the use of a more powerful laser, a longer path length, and a heated optical cell should also lead to improved sensitivity. Finally, increasing the dissolved gas extraction efficiency per unit time should help to alleviate sample size limitations and increase sample throughput. As mentioned, reconfiguration of the fluid sampling system to include a lower flow pump, alternate membrane inlet configurations, and a sediment probe (to enable profiling of porewater composition) will position this and similar technologies to advance our understanding of the relationship among physical, geochemical, and biological processes and their relative influences on elemental cycling.

ASSOCIATED CONTENT

Ⓢ Supporting Information
Additional text, figures, and table. This material is available free of charge via the Internet at http://pubs.acs.org.

AUTHOR INFORMATION

Corresponding Author
*E-mail: (S.D.W.) sdwankel@whoi.edu; (P.R.G.) pgirguis@oeb.harvard.edu.

Present Addresses
‖Department of Marine Chemistry and Geochemistry, Woods Hole Oceanographic Institution, Woods Hole, MA 02540.
⊥Department of Earth, Atmospheric and Planetary Sciences, Massachusetts Institute of Technology, Cambridge, MA 02139.

Notes
The authors declare no competing financial interest.

ACKNOWLEDGMENTS

REFERENCES

(1) Swinnerton, J.; Linnenbom, V.; Cheek, C. Determination of dissolved gases in aqueous solutions by gas chromatography. *Anal. Chem.* **1962**, *34* (4), 483−485.

(2) Swinnerton, J.; Linnenbom, V. Gaseous hydrocarbons in sea water: Determination. *Science* **1967**, *156* (3778), 1119−1120.

(3) Atkinson, L. P.; Richards, F. A. The occurence and distribution of methane in the marine environment. *Deep Sea Res. Oceanogr. Abstr.* **1967**, *14* (6), 673−684.

(4) Reeburgh, W. S. Determination of gases in sediments. *Environ. Sci. Technol.* **1968**, *2* (2), 140−141.

(5) Reeburgh, W. S. Oceanic Methane Biogeochemistry. *Chem. Rev.* **2007**, *107*, 486−513.

(6) Knittel, K.; Boetius, A. Anaerobic oxidation of methane: Progress with an unknown process. *Annu. Rev. Microbiol.* **2009**, *63*, 311−334.

(7) Bell, R. J.; Short, R. T.; van Amerom, F. H.; Byrne, R. H. Calibration of an In Situ Membrane Inlet Mass Spectrometer for Measurements of Dissolved Gases and Volatile Organics in Seawater. *Environ. Sci. Technol.* **2007**, *41* (23), 8123−8128.

(8) Camilli, R.; Duryea, A. N. Characterizing spatial and temporal variability of dissolved gases in aquatic environments with in situ mass spectrometry. *Environ. Sci. Technol.* **2009**, *43* (13), 5014−5021.

(9) Luther, G. W., III; Glazer, B. T.; Ma, S.; Trouwborst, R. E.; Moore, T. S.; Metzger, E.; Kraiya, C.; Waite, T. J.; Druschel, G.; Sundby, B.; Taillefert, M.; Nuzzio, D. B.; Shank, T. M.; Lewis, B. L.; Brendel, P. J. Use of voltammetric solid-state (micro)electrodes for studying biogeochemical processes: Laboratory measurements to real time measurements with an in situ electrochemical analyzer (ISEA). *Mar. Chem.* **2008**, *108* (3−4), 221−235.

(10) Short, R. T.; Fries, D. P.; Kerr, M. L.; Lembke, C. E.; Toler, S. K.; Wenner, P. G.; Byrne, R. H. Underwater mass spectrometers for in situ chemical analysis of the hydrosphere. *J. Am. Soc. Mass Spectrom.* **2001**, *12* (6), 676−682.

(11) Wankel, S. D.; Germanovich, L. N.; Lilley, M. D.; Genc, G.; DiPerna, C. J.; Bradley, A. S.; Olson, E. J.; Girguis, P. R. Influence of subsurface biosphere on geochemical fluxes from diffuse hydrothermal fluids. *Nat. Geosci.* **2011**, *4*, 461−468.

(12) Wankel, S. D.; Joye, S. B.; Samarkin, V.; Shah, S. R.; Friederich, G. E.; Melas-Kyriazi, J.; Girguis, P. R. New constraints on methane fluxes and rates of anaerobic methane oxidation in a Gulf of Mexico brine pool via in situ mass spectrometry. *Deep Sea Research II* **2010**, *57*, 2022−2029.

(13) Camilli, R.; Reddy, C. M.; Yoerger, D. R.; Van Mooy, B. A.; Jakuba, M. V.; Kinsey, J. C.; McIntyre, C. P.; Sylva, S. P.; Maloney, J. V. Tracking hydrocarbon plume transport and biodegradation at Deepwater Horizon. *Science* **2010**, *330*, 201−204.

(14) Hoefs, J. *Stable Isotope Geochemistry*, 6th ed.; Springer: Berlin-Heidelberg, 2010.

(15) Sharp, Z. *Principles of Stable Isotope Geochemistry*, 1st ed.; Pearson Prentice-Hall: Upper Saddle River, NJ, 2007.

(16) Kendall, C. *Isotope Tracers in Catchment Hydrology*, 1st ed.; Elsevier: Amsterdam, 1998; p 839.

(17) Schlesinger, W. H. *Biogeochemistry: An Analysis of Global Change*, 2nd ed.; Academic Press: London, 1997; p 588.

(18) Bowling, D. R.; Sargent, S. D.; Tanner, B. D.; Ehleringer, J. R. Tunable diode laser absorption spectroscopy for stable isotope studies of ecosystem-atmosphere CO_2 exchange. *Agric. Forest Meteorol.* **2003**, *118*, 1−19.

(19) Crosson, E. R.; Ricci, K. N.; Richman, B. A.; Chilese, F. C.; Owano, T. G.; Provencal, R. A.; Todd, M. W.; Glasser, J.; Kachanov, A. A.; Paldus, B. A.; Spence, T. G.; Zare, R. N. Stable isotope ratios using cavity ring-down spectroscopy: Determination of $^{13}C/^{12}C$ for carbon dioxide in human breath. *Anal. Chem.* **2002**, *74*, 2003−2007.

(20) Kasyutich, V.; Martin, P.; Holdsworth, R. An off-axis cavity-enhanced absorption spectrometer at 1605 nm for the $^{12}CO_2/^{13}CO_2$ measurement. *Appl. Phys. B: Lasers Opt.* **2006**, *85*, 413−420.

(21) Moyes, A. B.; Schauer, A. J.; Siegwolf, R. T.; Bowling, D. R. An injection method for measuring the carbon isotope content of soil carbon dioxide and soil respiration with a tunable diode laser absorption spectrometer. *Rapid Commun. Mass Spectrom.* **2010**, *24*, 894−900.

(22) Keppler, F.; Laukenmann, S.; Rinne, J.; Heuwinkel, H.; Greule, M.; Whiticar, M.; Lelieveld, J. Measurement of $^{13}C/^{12}C$ methane from anaerobic digesters: Comparison of optical spectrometry with continuous-flow isotope ratio mass spectrometry. *Environ. Sci. Technol.* **2010**, *44*, 5067−5073.

(23) Witinski, M.; Sayres, D.; Anderson, J. G. High precision methane isotopologue ratio measurments at ambient mixing ratios using integrated cavity output spectroscopy. *Appl. Phys. B: Lasers Opt.* **2011**, *102*, 375−380.

(24) Gagliardi, G.; Borri, S.; Tamassia, F.; Capasso, F.; Gmachi, C.; Sivco, D. L.; Baillargeon, J. N.; Hutchinson, A. L.; Cho, A. Y. A frequency-modulated quantum-cascade laser for spectroscopy of CH_4 and N_2O isotopomers. *Isot. Environ. Health Stud.* **2006**, *41* (4), 313−321.

(25) Uehara, K.; Yamamoto, K.; Kikugawa, T.; Toyoda, S.; Tsuji, K.; Yoshida, N. Precise isotope abundance ratio measurement of nitrous oxide using diode lasers. *Sens. Actuators, B* **2003**, *90* (1−3), 250−255.

(26) Waechter, H.; Mohn, J.; Tuzson, B.; Emmenegger, L.; Sigrist, M. W. Determination of N_2O isotopomers with quantum cascade laser based absorption spectroscopy. *Opt. Express* **2008**, *16* (12), 9239−9244.

(27) Zare, R. N.; Kuramoto, D. S.; Haase, C.; Tan, S. M.; Crosson, E. R.; Saad, N. M. High-precision optical measurements of $^{13}C/^{12}C$ isotope ratios in organic compouns at natural abundance. *Proc. Natl. Acad. Sci., U. S. A.* **2009**, *106* (27), 10928−10932.

(28) Sayres, D. S.; Pfister, L.; Hanisco, T.; Moyer, E.; Smith, J.; St. Clair, J.; O'Brien, A.; Witinski, M.; Legg, M.; Anderson, J. G. Influence of convection on the water isotopic composition of the tropical tropopause layer and tropical stratosphere. *J. Geophys. Res.* **2010**, *115*, D00J20.

(29) Schaeffer, S.; Miller, J.; Vaughn, B. H.; White, J.; Bowling, D. R. Long-term field performance of a tunable diode laser absorption spectrometer for analysis of carbon isotopes of CO_2 in forest air. *Atmos. Chem. Phys.* **2008**, *8*, 5263−5277.

(30) Berman, E. S.; Gupta, M.; Gabrelli, C.; Garland, T.; McDonnell, J. J. High-frequency field-deployable isotope analyzer for hydrological applications. *Water Resour. Res.* **2009**, *45*, W10201.

(31) Gülzow, W.; Rehder, G.; Schneider, B.; Schneider von Deimling, J.; Sadkowiak, B. A new method for continuous measurement of methane and carbon dioxide in surface waters using off-axis integrated cavity output spectroscopy (ICOS): An example from the Baltic Sea. *Limnol. Oceanogr.: Methods* **2011**, *9*, 176−184.

(32) Baer, D.; Paul, J.; Gupta, M.; O'Keefe, A. Sensitive absorption measurements in the near-infrared region using off-axis integrated-cavity-output spectroscopy. *Appl. Phys. B: Lasers Opt.* **2002**, *75* (2−3), 261−265.

(33) Dong, F.; Junaedi, C.; Roychoudhury, S.; Gupta, M. Rapid, online quantification of H_2S in JP-8 fuel reformate using near-infrared cavity-enhanced laser absorption spectroscopy. *Anal. Chem.* **2011**, *83* (11), 4132−4136.

(34) Le, L. D.; Tate, J.; Seasholtz, M. B.; Gupta, M.; Owano, T. G.; Baer, D.; Knittel, T.; Cowie, A.; Zhu, J. Development of a rapid on-line acetylene sensor for industrial hydrogenation reactor optimization using off-axis integrated cavity output spectroscopy. *Appl. Spectrosc.* **2008**, *62* (1), 59−65.

(35) Duan, Z.; Mao, S. A thermodynamic model for calculating methane solubility, density and gas phase composition of methane bearing aqueous fluids from 273 to 523K and from 1 to 2000 bar. *Geochim. Cosmochim. Acta* **2006**, *70* (13), 3369−3386.

(36) Dong, F.; Baer, D. *Development of a Field-Deployable Methane Carbon Isotope Analyzer*; EGU General Assembly, Vienna, Austria, May 2−7, 2010; Vienna, Austria, 2010; p 5583.

(37) Johnson, R. C.; Cooks, R. G.; Allen, T. M.; Cisper, M. E.; Hemberger, P. H. Membrane Introduction Mass Sepctrometry: Trends and Applications. *Mass Spectrom. Rev.* **2000**, *19*, 1−37.

(38) Overney, F. L.; Enke, C. G. A mathematical study of sample modulation at a membrane inlet mass spectrometer - Potential application in analysis of mixtures. *J. Am. Soc. Mass Spectrom.* **1995**, *7*, 93−100.

(39) LaPack, M. A.; Tou, J. C.; Enke, C. G. Membrane Mass Spectrometry for the Direct Trace Analysis of Volatile Organic Compounts in Air and Water. *Anal. Chem.* **1990**, *62*, 1265−1271.

(40) McNevin, D. B.; Badger, M. R.; Kane, H. J.; Farquhar, G. D. Measurement of (carbon) kinetic isotope effect by Rayleigh fractionation using membrane inlet mas spectrometry for CO_2-consuming reactions. *Funct. Plant Biol.* **2006**, *33*, 1115−1128.

(41) Futo, I.; Degn, H. Effect of sample pressure on membrane inlet mass spectometry. *Anal. Chim. Acta* **1994**, *294* (2), 177−184.

(42) Orange, D. L.; Yun, J.; Maher, N.; Barry, J.; Greene, G. Tracking California seafloor seeps with bathymetry, backscatter and ROVs. *Cont. Shelf Res.* **2002**, *22* (16), 2273−2290.

(43) Lorenson, T. D.; Kvenvolden, K. A.; Hostetter, F. D.; Rosenbauer, R. J.; Orange, D. L.; Martin, J. B. Hydrocarbon geochemistry of cold seeps in the Monterey Bay National Marine Sanctuary. *Mar. Geol.* **2002**, *181*, 285−304.

(44) LaBonte, A. L.; Brown, K. M.; Tryon, M. D. Monitoring periodic and episodic flow events at Monterey Bay seeps using a new optical flow meter. *J. Geophys. Res.* **2007**, *112*, B02105.

(45) Barry, J. P.; Greene, H. G.; Orange, D. L.; Baxter, C. H.; Robison, B. H.; Kochevar, R. E.; Nybakken, J. W.; Reed, D. L.; McHugh, C. M. Biologic and geologic characteristics of cold seeps in Monterey Bay, California. *Deep Sea Res., Part I* **1996**, *43* (11−12), 1739−1755.

(46) Martens, C. S.; Albert, D. B.; Alperin, M. J. Stable isotope tracing of anaerobic methane oxidation in the gassy sediments of Eckernförde Bay, German Baltic Sea. *Am. J. Sci.* **1999**, *299*, 589−610.

(47) Lapham, L. L.; Chanton, J. P.; Martens, C. S.; Sleeper, K.; Woolsey, J. R. Microbial activity in surficial sediments overlying acoustic wipeout zones at a Gulf of Mexico cold seep. *Geochem., Geophys., Geosyst.* **2008**, *9* (6), Q06001.

(48) Alperin, M.; Reeburgh, W. S.; Whiticar, M. Carbon and hydrogen fractionation resulting from anaerobic methane oxidation. *Global Biogeochem. Cycles* **1988**, *2* (3), 279−288.

(49) Alperin, M. J.; Hoehler, T. M. Anaerobic methane oxidation by archaea/sulfate-reducing aggregates: 2. Isotopic Constraints. *Am. J. Sci.* **2009**, *309*, 958−984.

(50) Lloyd, K. G.; Alperin, M. J.; Teske, A. Environmental evidence for net methane production and oxidation in putative ANaerobic MEthanotrophic (ANME) archaea. *Environ. Microbiol.* **2011**, *13* (9), 2548−2564.

(51) Holler, T.; Wegener, G.; Knittel, K.; Boetius, A.; Brunner, B.; Kuypers, M. M. M.; Widdel, F. Substantial $^{13}C/^{12}C$ and D/H fractionation during anaerobic oxidation of methane by marine consortia enriched *in vitro*. *Environ. Microbiol. Rep.* **2009**, *1* (5), 370−376.

(52) Kessler, J.; Reeburgh, W. S.; Tyler, S. C. Controls on the methane concentration and stable isotope (δ^2H-CH_4 and $\delta^{13}C$-CH_4) distributions in the water column of the Black Sea and Cariaco Basin. *Global Biogeochem. Cycles* **2006**, *20*, GB4004.

(53) Johnson, K.; Needoba, J. A.; Riser, S. C.; Showers, W. J. Chemical sensor networks for the aquatic environment. *Chem. Rev.* **2007**, *107*, 623−640.

(54) Shakhova, N.; Semiletov, I.; Salyuk, A.; Yusupov, V.; Kosmach, D.; Gustafsson, O. Extensive methane venting to the atmosphere from sediments of the East Siberian Artic Shelf. *Science* **2010**, *327* (5970), 1246−1250.